International Journal of Bridge Engineering (IJBE), Special Issue 2017, pp. 53-77

DUCTILITY WITHOUT CONFINEMENT A NEW DESIGN AND CONSTRUCTION APPROACH FOR RC BRIDGE COLUMNS

Abdullah Boudaqa[1], Mostafa Tazarv[2] and Ishtiaque Tuhin[3]

[1,2,3] South Dakota State University, Dept. of Civil and Env. Engineering, Brookings, SD, USA
e-mail: abdullah.boudaqa@jacks.sdstate.edu, mostafa.tazarv@sdstate.edu, ishtiaque.tuhin@jacks.sdstate.edu

ABSTRACT: Bridges are currently designed to withstand severe earthquakes without collapse. This design objective is usually attained by ensuring large ductilities for columns. For reinforced concrete (RC) columns, large displacement capacities can be achieved through confinement, which allows significant yielding of the column longitudinal reinforcement without premature failure of the core concrete. Concrete can be confined using transverse reinforcement or external jackets (e.g. steel tube or fiber reinforced polymer wrap). Therefore, ductility of RC columns depends on confinement. A new design approach for RC columns is proposed in the present study in which large displacement capacities can be achieved incorporating a new detailing without the direct need of confinement. First the proposed detailing is discussed, which incorporates (1) external reinforcing steel bars restrained against buckling to develop plastic bending moments, (2) a heavy-duty steel pipe connecting the column to the adjoining member through a pin connection to resist plastic shear forces, and (3) detachable mechanical bar splices. Second, the performance of buckling restrained reinforcement (BRR) is investigated through an experimental study and a simple design method is proposed for BRR. Finally, the seismic performance of the new column is investigated through extensive parametric study. The results showed that the displacement capacity of the proposed RC bridge columns can be more than twice that of conventional bridge columns. Furthermore, the column can be repaired with simple tools and minimal costs after a severe event since reinforcing steel bars are replaceable.

KEYWORDS: Buckling Restrained Reinforcement; Confinement; Ductility; RC Bridge Columns; Novel Columns.

1 INTRODUCTION

Bridges are currently designed to withstand severe earthquakes without collapse. This design objective is usually attained by providing large displacement capacities for columns. Accurate estimation of seismic demands

also plays a major role in a successful design. For reinforced concrete (RC) columns, large displacement capacities can be achieved through confinement, which allows significant yielding of the column longitudinal reinforcement without premature failure of the core concrete. Concrete can be confined using transverse reinforcement [1] or external jackets (e.g. steel jackets and tubes or fiber reinforced polymer (FRP) wrap and tubes) [e.g. 2-3]. In general, concrete sections confined with external jackets show higher strength and stiffness compared to transverse-steel confined sections. Furthermore, external jackets are easier to repair after an event compared to steel confined sections in which transverse steel bars are embedded in concrete. Displacement based design specifications such as the AASHTO Guide Specifications for LRFD Seismic Bridge Design Concrete (AASHTO SGS) [4], utilize displacement ductility as the main analysis and design measure. Therefore, ductility, the ratio of the column tip displacement to the effective yield displacement, is the most important design parameter for seismic applications. Energy dissipation mechanism, force capacities, and stability of bridges are also included in the design but as the secondary parameters [5].

Reduction of bridge column damage incorporating external devices (such as seismic isolators [e.g. 6]), advanced materials (such as high performance concrete and shape memory alloys [e.g. 7]), or innovative detailing (such as rocking mechanism [e.g. 8]) has been the focus of several studies. Seismic isolations are designed to keep bridge column seismic demands in the linear-elastic range minimizing the column damage. High performance concrete reduces the damage in plastic hinge regions. Shape memory alloys as the longitudinal bars significantly reduce permanent lateral deformations of bridge columns. Rocking columns, which usually include post-tensioning tendons and one kind of energy dissipater, exhibit minimal permanent lateral deformations and low damage. These and other studies confirmed that none- or low-damage RC bridge columns are feasible for field applications.

Accelerated bridge construction (ABC), which utilizes innovative detailing and new technologies to reduce the onsite activities, has been recently emphasized in the literature [e.g. 2, 7, 9, and 10]. ABC for bridge columns is more challenging than other components since the integrity of a bridge depends on the performance of the columns and their connections. ABC methods are considered successful when ABC components emulate the performance of cast-in-place components. However, none of the conventional cast-in-place or ABC column detailing found in the literature guarantee quick repair of bridge columns after strong earthquakes, if the repair is needed.

Recent studies were successful in combining the advantages of ABC and low-damage scheme [e.g. 7, 9, and 10]. However, the repair, if needed, is not usually easy and cost-effective. For example, yielded tendons in rocking columns [e.g. 8] are hard to repair or replace. If rocking columns incorporate internal energy dissipaters, it would be impractical to replace them. To repair

one module of modular bridge columns [e.g. 9], the bridge superstructure should be jacked up, the damaged module should be removed, and reinforcement/tendons may be replaced to complete the repair. This type of repair is tedious and time-consuming. No study was found in the literature that allows replacing the damaged components of modular RC bridge columns, specifically reinforcement, within hours after an earthquake with minimal repair costs and effort.

A new construction and design approach for RC bridge columns is proposed in the present study in which large displacement capacities can be achieved without the direct need of confinement incorporating an innovative detailing. The proposed detailing also allows replacement of damaged reinforcement through disassembly. Furthermore, the proposed novel column is fully precast in-line with ABC.

The main goals of the present study are (1) to accelerate construction using fully precast columns, (2) to improve displacement capacity, and (3) to limit the damage to replaceable reinforcement, which allows minimizing the repair time and eliminating the total bridge replacement through component disassembly.

First, the detailing of proposed novel column is illustrated for a column-to-footing connection. Then, the components of the new detailing are briefly discussed. A summary of modeling methods to analytically investigate the behavior of the novel column is presented. Finally, the results of analytical studies including force-displacement relationships, failure modes, and displacement ductility capacities of the novel column are represented.

2 PROPOSED NOVEL COLUMN DETAILING

Figure 1 illustrates the detail of a typical conventional cast-in-place column and the proposed novel column for a column-to-footing connection. Conventional reinforced concrete bridge columns (Fig. 1a) consist of core concrete, cover concrete, and longitudinal and transverse reinforcement. The ductility capacity of a conventional column is attained through the use of confining (transverse) reinforcement, and the strength of the column is provided by the core concrete strength and the amount and type of the longitudinal reinforcement. Figure 1b shows the main components of the proposed detailing, which includes (1) a fully precast column with exposed longitudinal dowels, (2) a shear pin made of steel pipe to be inserted into a steel cup placed in the footing, (3) mechanical bar splices, which are commonly referred to as couplers, that can be detached, (4) external reinforcement restrained against buckling (BRR) to connect the precast column dowels to the footing dowels, and (5) a steel plate between the precast column and the footing to prevent damage during rocking. All components are designed as capacity protected members except BRR, which is allowed to yield and fracture. The proposed column is repairable since the exposed reinforcement, BRR, can be replaced after a severe event without the

use of any other repair methods such concrete replacement, patching, jacketing, etc.

A few studies proposed repair methods for bridge columns with ruptured reinforcement [11-12]. However, those repair methods are not as easy as the proposed novel column repair since the concrete have to be removed, new reinforcement should be spliced to existing bars, and then a new concrete/grout should be poured to complete the repair. The repair proposed in the present study is simply done by replacing BRR.

Tazarv and Saiidi [13] recommended five coupler types for bridge columns: shear-screw, headed, threaded, swaged, and grouted couplers. Of which, headed and threaded couplers are suitable for the proposed detailing (Fig. 1b) since (1) they can fracture anchoring bars outside the coupler region, (2) they can be attached/detached using simple tools such as pipe-wrenches, and (3) they are relatively small to fit into the reduce section of the column.

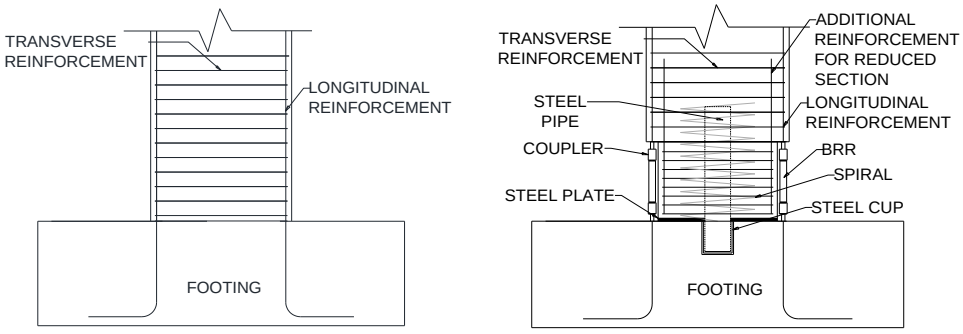

(a) Conventional bridge column detailing (b) Proposed novel column detailing

Figure 1. Conventional versus repairable RC bridge columns

The precast column in the proposed detailing can be designed using current codes (e.g. AASHTO LRFD [14]). A heavy-duty steel pipe embedded in the column is used as a pin to provide shear resistance. The steel pipe can be extended into the adjacent element (bent cap or footing) where a steel cup is embedded. A gap between the pipe and the cup will allow rotation of the pipe inside the cup. However, long pipes and minimal gaps result in dual-curvature deformations for the pipe making the joint partially fixed. The performance of shear pipe-pin was experimentally and analytically investigated by Zaghi and Saiidi [15]. Shear pipe-pin design guidelines proposed in [15] were adopted in the present study.

Detachable mechanical bar splices are utilized to connect the precast column longitudinal reinforcement, BRR, and the adjoining member reinforcement. A steel plate can be used at the interface of the two concrete members to avoid damage of concrete during lateral movements.

Exposed reinforcing steel bars cannot resist compressive forces since they buckle at low compressive loads. Therefore, they should be restrained against buckling. Two different types of buckling restrained reinforcement (BRR) can be incorporated in the proposed repairable bridge column: (1) BRR without any section reduction (Fig. 2), and (2) dog-bone BRR (Fig. 3), which is referred to as BRRD hereafter. In BRR, the total length of the bar is allowed to yield while the reinforcement will mainly yield in the reduced sections of BRRD. Adjoining bars at the ends of BRR can be oversized to prevent yielding and to limit the damage to only BRR. It should be noted that BRR in the proposed joint detailing (Fig. 1b) are to resist the external moments through withstanding both tensile and compressive stresses.

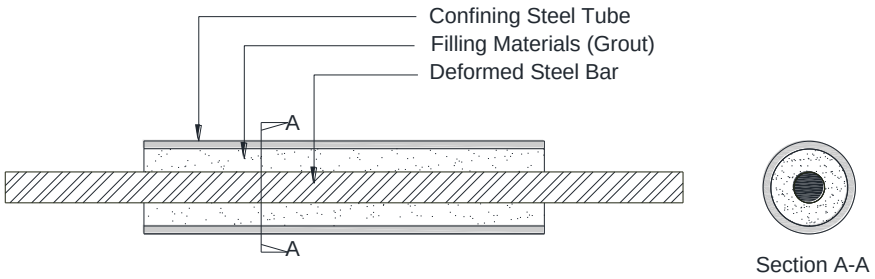

Figure 2. Buckling restrained reinforcement (BRR)

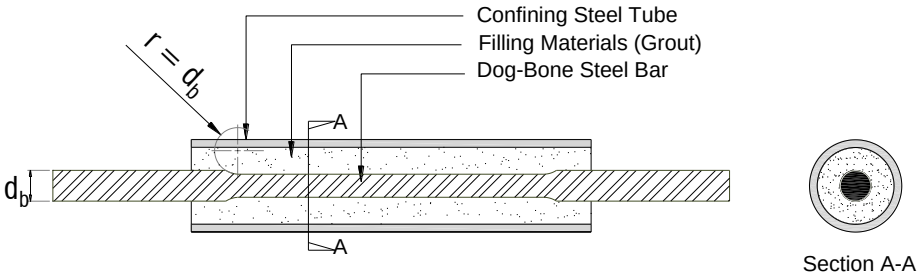

Figure 3. Dog-bone buckling restrained reinforcement (BRRD)

2.1 Buckling restrained reinforcement

External reinforcing bars have been used in previous studies to increase energy dissipation of rocking columns [10, 12, 16, and 17] and post-tensioned concrete buildings [18]. Only BRRD (Fig. 3) have been used in the previous studies. Furthermore, the steel bars used in BRRD were not usually conventional reinforcing steel bars (Grade 60 ASTM A615 or A706) allowed by current bridge and building codes. With some modification, the external energy dissipaters can be used as the longitudinal reinforcement of RC members as exposed bars for the ease of repair. The feasibility and performance of a new type of external energy dissipater, BRR (Fig. 2), were experimentally

investigated in the present study, and are discussed in the following section.

2.1.1 BRR experimental program

As mentioned in the previous section, dog-bone energy dissipaters showed promising performance in the past studies [10, 12, 16, and 17]. In an attempt to avoid bar machining and to reduce the cost, the feasibility and performance of conventional reinforcing steel bars without any section reduction enclosed in tubes were investigated by testing 16 specimens under axial compressive loading at the Lohr Structures Laboratory at South Dakota State University. Test matrix, procedure, and a summary of the BRR test results are presented herein.

2.1.1.1 BRR test specimens

A total of 16 specimens (Table 1) including four reference deformed bars, three deformed bars restrained with a series of steel nuts, and nine BRR were constructed and tested under monotonic and cyclic axial compressive loading to failure. Two different sizes of deformed steel bars, No. 4 (Ø13 mm) and No. 8 (Ø25 mm), were used in this experimental investigation. Furthermore, three slenderness ratios for BRR were included in the experiment: 10, 15, and 20. The BRR slenderness ratio is defined as the ratio of the tube length to the bar diameter. The length of the reference bars (unrestrained against buckling) was based on the total length of their corresponding BRR. Grout filled steel tubes with different geometries were used to prevent buckling of reinforcement. The main purpose of using the grout is to increase the moment of inertia of the section and to enhance the durability. Loading for all specimens was monotonic except "No4-BL14.81d-TL7.5s-TG13-G0.50," which was cyclic. Guide on the specimen naming system is presented in the table footnote.

Table 1. Test matrix for buckling restrained reinforcement

Specimen ID	Bar No. (mm)	Bar Length, in. (mm)	Tube O.D., in. (mm)	Tube Gage	Tube Length, in. (mm)	Filler	Peak Stress, ksi (MPa)	Strain at Peak Stress (in./in.)
No4-BL11.00d	4 (Ø13)	11.00 (279.4)	N.A.	N.A.	N.A.	N.A.	23.45 (161.7)	0.005
No4-BL10.94d	4 Ø13)	11.00 (279.4)	N.A.	N.A.	N.A.	N.A.	21.06 (145.2)	0.003
No8-BL16.91d	8 (Ø25)	16.96 (430.8)	N.A.	N.A.	N.A.	N.A.	51.48 (354.9)	0.007
No8-BL10.25d	8 (Ø25)	10.25 (260.4)	N.A.	N.A.	N.A.	N.A.	53.19 (366.7)	0.008
No4-BL11.00d-Nuts-G0.875	4 (Ø13)	11.00 (279.4)	N.A.	N.A.	N.A.	Steel Nuts	28.14 (194)	0.005
No4-BL11.00d-Nuts-G0.42	4 (Ø13)	11.00 (279.4)	N.A.	N.A.	N.A.	Steel Nuts	40.46 (279)	0.034
No4-BL11.00d-Nuts-G0.20	4 (Ø13)	11.00 (279.4)	N.A.	N.A.	N.A.	Steel Nuts	144.71 (997.7)	0.034
No4-BL11.00d-TL5.0s-TG18-G3.00	4 (Ø13)	11.00 (279.4)	1 ¼ (31.8)	18 GA	5 (127)	Grout	42.46 (292.7)	0.021
No4-BL10.94d-TL5.0s-TG16-G2.94	4 (Ø13)	10.94 (277.9)	1 ¼ (31.8)	16 GA	5 (127)	Grout	68.61 (473)	0.033
No4-BL12.28d-TL7.5s-TG16-G0.50	4 (Ø13)	12.06 (320)	1 ¼ (31.8)	16 GA	7.5 (190.5)	Grout	168.03 (1158.5)	0.062
No4-BL12.20d-TL7.5s-TG14-G0.50	4 (Ø13)	12.20 (209.9)	1 ¼ (31.8)	14 GA	7.5 (190.5)	Grout	222.97 (1537.3)	0.078
No4-BL14.81d-TL7.5s-TG14-G0.50	4 (Ø13)	14.81 (376.2)	1 ¼ (31.8)	14 GA	10 (254)	Grout	196.24 (1353)	0.052
No4-BL14.81d-TL7.5s-TG13-G0.50	4 (Ø13)	14.81 (376.2)	1 ¼ (31.8)	13 GA	10 (254)	Grout	191.63 (1321.2)	0.056
No8-BL14.56d-TL10.0s-TG13-G0.50	8 (Ø25)	14.56 (369.8)	2 ¼ (57.2)	13 GA	10 (254)	Grout	150.04 (1034.5)	0.113
No8-BL17.00d-TL10.0s-TG11-G1.00	8 (Ø25)	17.00 (431.8)	2 ¼ (57.2)	11 GA	10 (254)	Grout	112.2 (773.6)	0.064
No8-BL19.62d-TL15.0s-TG11-G0.50	8 (Ø25)	19.62 (498.3)	2 ¼ (57.2)	11 GA	15 (254)	Grout	Setup Limit	Setup Limit

Note: Guide for Specimen Identification:
Example: No4-BL10.94d-TL5.0s-TG16-G0.5
First Term-Bar Size: No4 or No8. (e.g. No4 means No. 4 reinforcing bar).
Second Term-Bar Length and Deformation Type (d for deformed and p for plain). (e.g. BL10.94d means the length of deformed reinforcing bar is 10.94 in.).
Third Term-Tube Length and Material (s for steel, a for aluminum). (e.g. TL5.0s means the length of steel tube is 5.0 in.).
Fourth Term-Tube Gage: (e.g. TG16 means the tube gage is 16).
Last Term-Total Gap at the Ends of the Reinforcement: (e.g. G0.5 means the total gap is 0.5 in.

2.1.1.2 BRR material properties

Each BRR is made of three components: (1) reinforcing steel bar, (2) steel tube, and (3) filler material. Constitutive materials of each component were tested according to ASTM standards and a summary of the material properties is presented herein:

- Reinforcing Steel Bar: ASTM A706 Grade 60 deformed steel bars were used in BRR. The measured yield and ultimate strengths of the bar were 77.25 ksi (532.6 MPa) and 118.25 ksi (815.3 MPa), respectively.
- Steel Tube: Tubes encasing reinforcing bars were made of ASTM A513 Grade 1026 carbon steel. The yield and the ultimate strengths of the steel tubes were 66 ksi (455 MPa) and 75 ksi (517.1 MPa), respectively.
- Non-Shrink Grout: Conventional non-shrink fine-aggregate high-flow grout was used to fill the gap between reinforcing bars and steel tubes. The test-day measured compressive strength of the grout was 6.78 ksi (46.8 MPa) to 10.19 ksi (70.3 MPa).

2.1.1.3 BRR test setup and instrumentation

Three ASTM A36 steel plates each with a thickness of 1 in. (25 mm) connected with four post-tensioning rods were utilized in a self-reacting compressive setup (Fig. 4). Steel cups at the center of the two steel plates were to hold the specimens and to ensure that the specimens are secure during the compressive test.

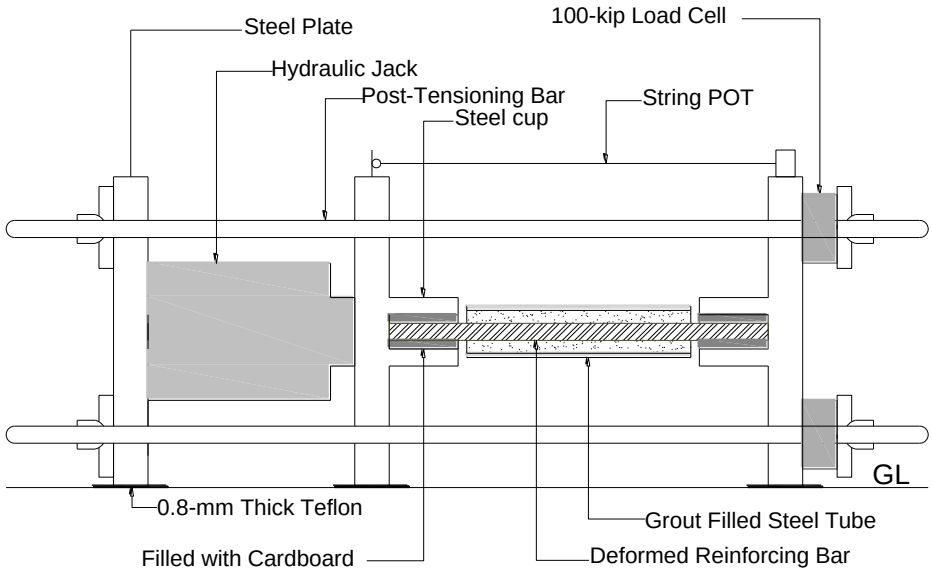

Figure 4. Elevation view of BRR test setup

A hydraulic hollow-core jack was used to apply compressive monotonic and cyclic loads and was controlled with a manual oil pump. The average displacement rate was 0.0052 in./sec (0.13 mm/sec). Four 100-kip (444.8-kN) load cells and three string potentiometers (POT) were used to measure forces and displacements of BRR, respectively.

2.1.2 BRR experimental results

The specimens were tested according to the details presented in the previous section. A summary of the test results is presented herein.

2.1.2.1 BRR failure mechanism

Figure 5a shows the failure mode of a reference deformed No. 4 bar with a total length of 11 in. (279 mm or 22 times the bar diameter, d_b) under compression in which the No. 4 bar buckled at a compressive stress of 23.45 ksi (161.7 MPa). In an attempt to improve the bar buckling resistance, bars were passed through a series of steel hex nuts. The gap between the nuts and the face of the steel cups in the axial direction (Fig. 4) was varied by changing the number of the nuts.

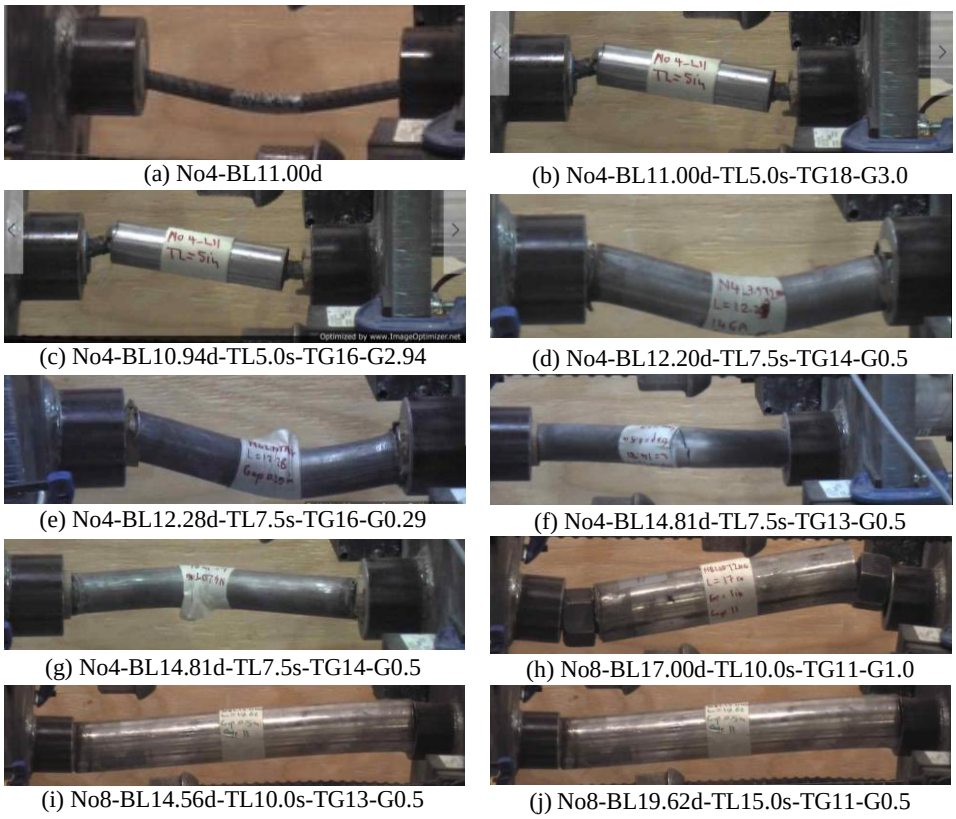

(a) No4-BL11.00d

(b) No4-BL11.00d-TL5.0s-TG18-G3.0

(c) No4-BL10.94d-TL5.0s-TG16-G2.94

(d) No4-BL12.20d-TL7.5s-TG14-G0.5

(e) No4-BL12.28d-TL7.5s-TG16-G0.29

(f) No4-BL14.81d-TL7.5s-TG13-G0.5

(g) No4-BL14.81d-TL7.5s-TG14-G0.5

(h) No8-BL17.00d-TL10.0s-TG11-G1.0

(i) No8-BL14.56d-TL10.0s-TG13-G0.5

(j) No8-BL19.62d-TL15.0s-TG11-G0.5

Figure 5. Failure of BRR specimens

It was found that the compressive behavior of a nut-encased reinforcement is the same as that of the unrestrained steel bar (Fig. 5a) if the gap is not filled during the testing (or when the gap is large). Furthermore, a reinforcing steel bar can be restrained against buckling and the compressive strength can exceed the yield strength of the bar if the total gap in the series of the nuts does not exceed $0.5d_b$. Based on these findings, nine BRR were subsequently tested to failure to further validate the initial findings and to investigate the compressive performance.

Figure 5 shows failure modes of the nine BRR specimens under compressive loads. For No. 4 BRR, the device buckled at very large stresses [200 ksi (1379 MPa)] where the total axial gap between the tube and the cup was not more than $0.5d_b$. For cases in which the gap was more than $0.5d_b$, the specimen deformed in a "Z-shape" manner (Fig. 5b and c). Larger gaps resulted in lower compressive strength before bucking. Similar to No. 4 BRR, No. 8 BRR showed large compressive stresses before failure when the total axial gap was $0.5d_b$.

In summary, it was found that a short BRR exhibits higher compressive stress and strain capacities compared to a long BRR with the same properties. BRR with thicker tubes achieve higher stress and strain capacities compared to those with thinner tubes. Finally, the axial gap between the tube and the support plays a significant role to control the compressive behavior of BRR. This gap should be limited to one half of the bar diameter. In depth discussion of the BRR test results and findings can be found in Tuhin [19].

2.1.2.2 BRR stress-strain relationships

Figure 6 shows stress-strain relationships of all buckling restrained reinforcement and the reference bars. It can be seen that the unrestrained steel bars buckled under low compressive stresses (less than the yield strength). Also, with proper detailing (e.g. minimal total axial gap, sufficient tube diameter, and tube wall thickness), it is possible to achieve large stress and strain capacities for the proposed buckling restrained reinforcement. Note the dashed horizontal lines in Fig. 6 are the measured tensile yield and ultimate strength for the steel bars used in BRR assuming that the steel bar stress-strain behavior is symmetric in tension and compression.

The compressive stress of BRR can exceed the ultimate strength of the bar because of the contribution of the tube/grout after the gap closure. The compressive strain at the peak stress can exceed 5%, which will be sufficient in most practical cases since the strain of compressive reinforcement in a concrete section is usually controlled by the core concrete strains. The core concrete strain capacity even in a highly confined section does not exceed 5%.

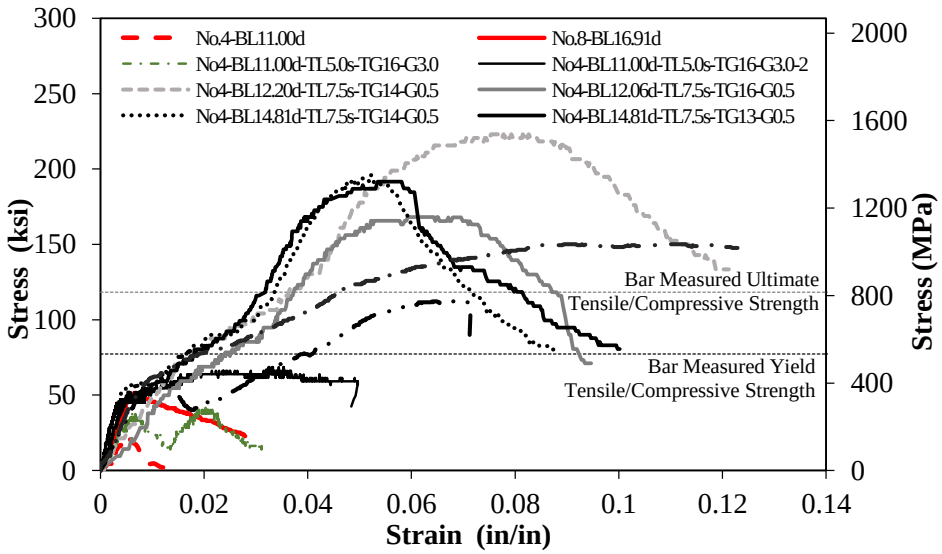

Figure 6. Stress-strain relationships for buckling restrained reinforcement

Furthermore, it can be seen that the total axial gap is a critical parameter to control the behavior of BRR, and should not exceed one half of the bar diameter. Additionally, it was found that the tube thickness has insignificant effect on the BRR performance if tubes are designed properly (Refer to Section 2.1.3 for a conservative design method for BRR).

Only one No. 4 BRR was tested under cyclic loading to failure. The test results confirmed that BRR also exhibits large compressive stress and strain capacities under cyclic loads without low-cycle fatigue. The envelope of the BRR cyclic stress-strain hysteresis was the same as the stress-strain relationship of a same BRR but tested under the monotonic loading.

2.1.3 Proposed design method for BRR

Sarti et al. [20] investigated the compressive behavior of BRRD through experimental and analytical studies. They quantified the initial stiffness of BRRD and proposed an equation to estimate the buckling force of the device. However, no systematic method of the design of BRRD was proposed. A simple design method for both BRR and BRRD was developed in the present study and is summarized herein.

Figure 7 shows BRR/BRRD design parameters assuming that the tube is not filled with grout. In this case, bar will locally buckle under compressive loads until touching the inner side of the tube causing bending of the tube as a beam. Based on the experimental findings, BRR/BRRD with a longitudinal gap of half the bar diameter ($0.5d_b$) or less will fail at very high stresses (twice the ultimate strength of the bar) thus other modes of failure (e.g. Z-shape bending) is

prevented meeting this gap requirement.

It can be assumed that the steel bar inside the tube acts as a truss element. Therefore, three plastic hinges are needed to make the bar unstable. It was assumed that two hinges are at the locations where the bar buckles (Fig. 7b and c) inside the tube and one hinge forms on the bar at the middle of the tube.

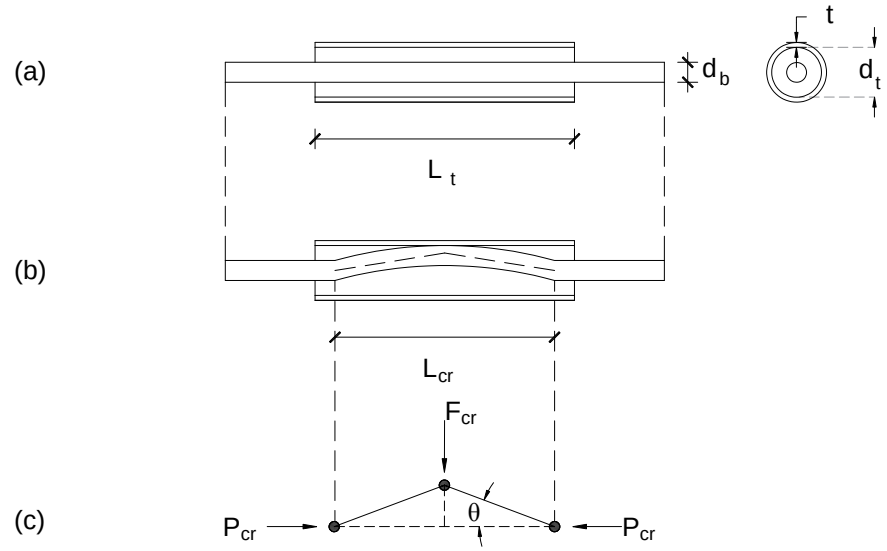

Figure 7. Design parameters for buckling restrained reinforcement

The buckling load of a bar can be estimated using the Euler's buckling equation:

$$P_{cr} = \frac{\pi^2 \mathrm{EI}}{(KL)^2} \tag{1}$$

where E is the modulus of elasticity of the bar, I is the moment of inertia of the bar, L is the length of the bar, and K is the effective length factor. K=1 for pinned-pinned elements, thus, the critical length required to cause bar buckling is

$$L_{cr} = \sqrt{\frac{\pi^2 \mathrm{EI}}{P_{cr}}} \tag{2}$$

The maximum possible compressive strength of a bar is equal to the plastic force of the bar, which is the product of the bar area (A_b) and the bar ultimate stress (f_{ub}), which was conservatively assumed to be 1.5 times the yield strength (f_{yb}) for ASTM A706 and ASTM A615 bars. These two types of reinforcement are extensively utilized in buildings and bridges.

$$P_{cr} = A_b \times f_{ub} = 1.5 \times A_b \times f_{yb} \tag{3}$$

Substituting Eq. 3 in Eq. 1

$$L_{cr} = \sqrt{\frac{\pi^2 \mathrm{EI}}{1.5 A_b \cdot f_{yb}}} = 0.64 d_b \sqrt{\frac{\mathrm{E}}{f_{yb}}} \tag{4}$$

Since the bar is enclosed in a tube, it can be assumed that there is a resisting vertical force (F_{cr} in Fig. 7c) at the middle hinge when the vertical gap between the inner side of the tube and the bar is closed (assuming there is no grout). The maximum vertical displacement of the bar before touching the tube can be obtained from the geometry. A relationship between P_{cr} and F_{cr} can be determined using the equilibrium at the truss joint as:

$$F_{cr} = 2P_{cr} \times \tan(\theta) = 2P_{cr} \times \frac{d_t - d_b}{L_{cr}} \tag{5}$$

where d_t is the inner tube diameter. By substituting Eq. 4 in Eq. 5:

$$F_{cr} = 3.1 P_{cr} \frac{d_t - d_b}{d_b} \sqrt{\frac{f_{yb}}{E}} \tag{6}$$

The lateral load on the tube (F) tends to bend the tube. The maximum bending stress can be assumed to be equal to the yield stress of the tube (f_{yt}):

$$f_{yt} = \frac{M}{S_{xt}} \tag{7}$$

where M is the bending moment at the mid-length of the tube ($F_{cr}.L_t/4$), L_t is the length of the tube, and S_{xt} is the tube section modulus. By substituting Eq. 6 in Eq. 7:

$$S_{xt-demand} = \frac{F_{cr} L_t}{4 f_{yt}} \tag{8}$$

From strength of material, $S_{xt} = I_t / y_t$ where I_t is the tube moment of inertia and $y_t = (d_t+2t)/2$ for a tube, where t is the wall-thickness of the tube. The tube section modulus can be expressed as:

$$S_{xt-capacity} = \frac{\pi[(d_t + 2t)^4 - d_t^4]}{32(d_t + 2t)} \tag{9}$$

Knowing the geometrical and mechanical properties for the bar and the tube, the tube thickness (t) for any bar diameter (d_b) can be estimated by equating Eq. 8 with Eq. 9. Alternately, any tube thickness that results in $S_{xt\text{-}capacity}$ greater than $S_{xt\text{-}demand}$ can be used for BRR.

2.1.4 Design methodology validation

The results of the BRR tests (Section 2.1.2) were used to validate the proposed BRR design methodology. Since the mechanical properties of the steel bars and tubes were known, the critical buckling load for each BRR was calculated using the design methodology discussed in section 2.1.3 and compared to the measured peak load for the corresponding specimen (Table 2). Note the proposed design method only includes the cases where BRR buckles but not Z-shape bending thus they are not reported in the table. It can be concluded that the calculated BRR capacities are always smaller than those measured in the tests indicating that the proposed design method is conservative and may be used to determine the tube sizes. The proposed method is conservative since the contribution of grout to the BRR strength was not included.

Table 2. Measured and calculated buckling forces for buckling restrained reinforcement

Specimen ID	Bar Dia., in. (mm)	Tube Length, in.(mm)	Measured Peak Load, kips (kN)	Calculated Peak Load, kips (kN)
No4-BL12.28d-TL7.5s-TG16-G0.5	0.5 (12.7)	7.5 (190.5)	33.60 (149.46)	12.52 (55.69)
No4-BL12.20d-TL7.5s-TG14-G0.5	0.5 (12.7)	7.5 (190.5)	44.59 (198.34)	15.91 (70.77)
No4-BL14.81d-TL7.5s-TG14-G0.5	0.5 (12.7)	7.5 (190.5)	39.24 (174.54)	15.91 (70.77)
No4-BL14.81d-TL7.5s-TG13-G0.5	0.5 (12.7)	7.5 (190.5)	38.33 (170.50)	19.45 (86.51)
No8-BL14.56d-TL10.0s-TG13-G0.5	1.0 (25.4)	10.0 (254)	118.53 (527.24)	55.41 (246.47)
No8-BL17.00d-TL10.0s-TG11-G1.0	1.0 (25.4)	10.0 (254)	88.63 (394.24)	75.14 (334.24)

3 ANALYTICAL INVESTIGATION

The seismic performance of conventional RC bridge columns and repairable precast columns is investigated through analytical studies. This section is dedicated to finite element modeling methods for the two column types.

3.1 Design of RC and repairable columns

Twenty seven RC bridge columns (e.g. Fig. 1a) were designed according to the AASHTO SGS [4] with three key variables: the aspect ratio (AR= 4, 6, and 8), the axial load applied to the column (5%, 10%, and 15% of the product of the column cross sectional area and the column concrete strength, or the axial load index – ALI), and the displacement ductility capacity, (μ = 3, 5, and 7). Different transverse reinforcing steel bars were used to achieve the target displacement ductility capacities. The diameter of all the columns was 48 in. (1219 mm), to minimize the variations. ASTM A706 Grade 60 reinforcing steel

bars were assumed for both longitudinal and transverse reinforcement. The compressive strength of concrete was 5000 psi (34.5 MPa) and the concrete cover was 2 in. (51 mm).

The displacement capacity is defined as a displacement where (1) the column core concrete fails, (2) the column longitudinal reinforcement fractures, or (3) the column lateral load carrying resistance drops by 15% with respect to the peak lateral load. The displacement ductility capacity is defined as the ratio of the column displacement capacity to the effective yield displacement according to the AASHTO SGS. The drift ratio is defined as the column lateral displacement to the column height. The aspect ratio is the ratio of the column height to the column largest side dimension (or diameter).

The aforementioned 27 RC bridge columns were modified based on the proposed detailing for the repairable precast bridge columns (section 2). Figure 8 shows the details of a typical repairable precast bridge column. Note that for repairable columns only the construction detailing was modified and the overall geometry, reinforcement, and material properties of the two column types were the same. In addition to the three main variables discussed for the RC columns, the yielding length of BRR was varied with respect to the analytical plastic hinge length ($0.25L_p$, $0.5L_p$, $0.75L_p$, and $1.0L_p$). The plastic hinge length for the RC columns with the aspect ratios of 4, 6, and 8 were 26.9 in. (683 mm), 34.5 in. (877 mm), and 42.2 in. (1072 mm), respectively.

In the repairable precast bridge columns, the column diameter at the column base was reduced from 48 in. (1219 mm) to 40 in. (1016 mm) to align BRR with the column longitudinal reinforcement. Minimal longitudinal reinforcement was provided in the reduced column section to avoid compressive failure. Transverse reinforcement with a spacing of 3 in. (resulting in a volumetric transverse steel ratio of 2%) was provided in the reduced section to increase the confinement and to eliminate any concrete damage in compression. A steel plate was placed between the column and the footing to avoid concrete damage.

As discussed before, two techniques can be used to localize the yielding to the BRR and to avoid yielding of the longitudinal reinforcement at the ends of a BRR: (1) utilize oversized reinforcement at the ends of BRR, and (2) use dog-bone BRR (BRRD). In the former case, the yielding length of BRR is the total length. For the latter case, the yielding length is the length of the reduced section.

The area in the yielding portion of each BRR was assumed to be the same as the area of the longitudinal reinforcement in the corresponding conventional RC bridge column. A steel pipe was incorporated at the column-to-footing interface to transfer the shear forces. The design of the shear pin was based on the guidelines proposed by Zaghi et al. [15]. It was found that a steel tube with an area of 15 in^2 (9677 mm^2) provides a shear capacity of 271.5 kips (1207.7 kN), which is sufficient for all repairable precast bridge column models. No. 4

(Ø13 mm) spirals with a spacing of 4 in. (102 mm) was placed around the steel pipe to improve the confinement. Finally, the compressive strength of concrete was assumed to be 5000 psi (34.5 MPa) and the concrete cover was 2 in. (51 mm), similar to the reference RC columns.

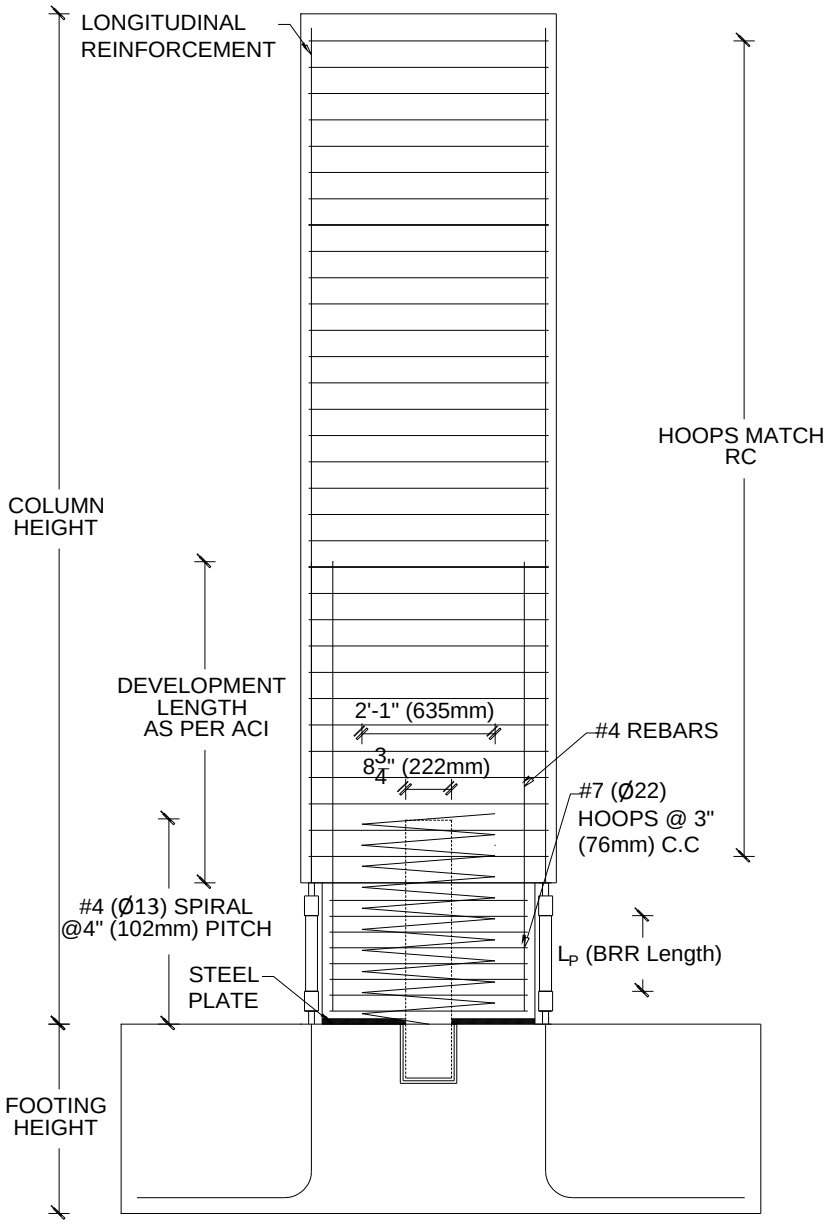

Figure 8. Typical repairable precast bridge columns

3.2 Modelling methods

Conventional RC bridge columns were modelled based on the modeling method presented and verified in Tazarv and Saiidi [7]. OpenSees [21] was used for the design and analysis of conventional RC columns. A three-dimensional fiber-section model was utilized for RC columns in which the "forceBeamColumn" element with five integration points (distributed plasticity) was used to model the column element. The concrete cover and core fibers were modeled using "Concrete01" and "Concrete04" material models, respectively. A uniaxial material, "ReinforcingSteel", was used to simulate the column reinforcement behavior. A fiber section with 30 circular and 10 radial segments was used to model both confined and unconfined concrete within the column section. Fibers for reinforcing steel bars were also included . Mander's model [1] was utilized to calculate properties of the confined concrete. Since shear and torsional stiffness are not included in fiber-section models, they were aggregated to the section in the first integration point of the column model (at the base) to make the model stable.

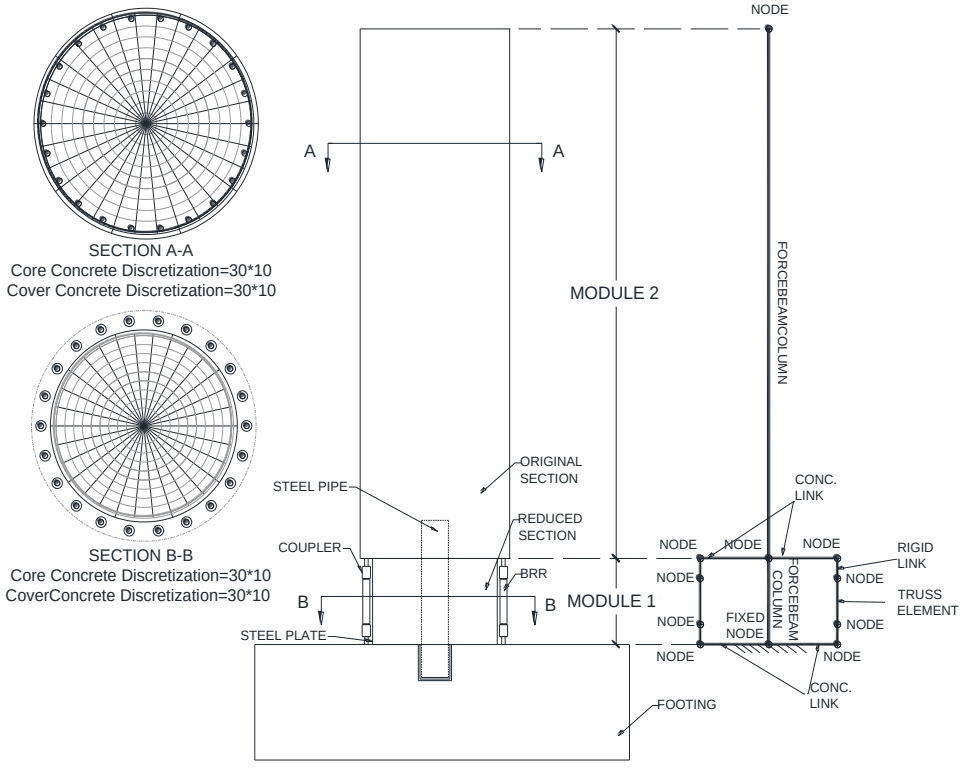

Figure 9. Repairable precast bridge column analytical model

Similar to conventional RC bridge columns, a three-dimensional fiber-section finite element model was developed to investigate the performance of repairable precast columns (Fig. 9). OpenSees was used for modeling. The column model can be generally divided into two submodules. The first module represents the portion of the column (reduced section, sec. B-B in Fig. 9) where yielding and damage of reinforcement are allowed. The second module is assumed to be damage-free (sec. A-A in Fig. 9). A "forceBeamColumn" element with five integration points was used to model the column elements in both modules. Since there was no longitudinal reinforcement inside the reduced column section to be extended into the footing (not developed), there was no reinforcement fiber inside this section. The stiffness of the shear pin was aggregated with the section at the first integration point of module 1 (at the base). A uniaxial material model, "ReinforcingSteel", was used to simulate all reinforcing steel bars. The replaceable reinforcement between the two couplers, which can be either BRR or BRRD, was modeled using a truss element with "ReinforcingSteel" material. The reinforcement between BRR and the adjacent concrete edge was modeled as a rigid link to incorporate the rigidity of the couplers. Finally, the external reinforcement (BRR or BRRD) was connected to the column and the footing using horizontal elastic elements with properties the same as those of the confined concrete (concrete links in Fig. 9).

Fiber sections with 30 circular and 10 radial segments were used to model the confined concrete within the two modules of the column element. The unconfined concrete was modeled with 10 circular and 10 radial segments. The axial load was applied to the top node of the column. The $P-\Delta$ effect was included in all analysis. The lateral load was applied at the top node of the column using a displacement control method. Each column model was pushed to failure. The column models were fixed against all translational and rotational degrees of freedom at the base level.

3.2.1 Repairable column modelling method validation

No test data is available for the proposed repairable bridge columns. However, a few experimental studies investigated the cyclic behavior of hybrid rocking columns (defined as columns with unbonded post-tensioned tendons and internal or external reinforcement as energy dissipaters) with external energy dissipaters. Of which, column model HBD3 discussed in Marriott et al. [16] was selected for further study. HBD3 had four unbonded post-tensioning tendons and four external energy dissipaters, two on each side of the square column. The column side dimension was 13.78 in. (350 mm) and the column height was 63 in. (1600 mm). The column was post-tensioned with a total force of 67.44 kips (300 kN). The column axial load due to dead load was 44.96 kips (200 kN) included in the posttensioning force. The test-day compressive strength of the column concrete was 7847 psi (54.1 MPa). The yield and the

ultimate strength of the external energy dissipaters (BRRD) were 46.4 ksi (320 MPa) and 66.7 ksi (460 MPa), respectively.

An analytical model similar to that discussed in the previous section was developed in OpenSees to simulate the force-displacement relationship of the hybrid column. Since HBD3 was a post-tensioned column, an additional "corotational truss" element at the center of the column model was added to represent the tendons. Note the repairable bridge column proposed in this study (Fig. 8) is not post-tensioned.

Figure 10 shows the measured and calculated force-displacement relationships for HBD3. It can be seen that there is a good agreement between the measured and calculated response indicating robustness of the proposed modeling method.

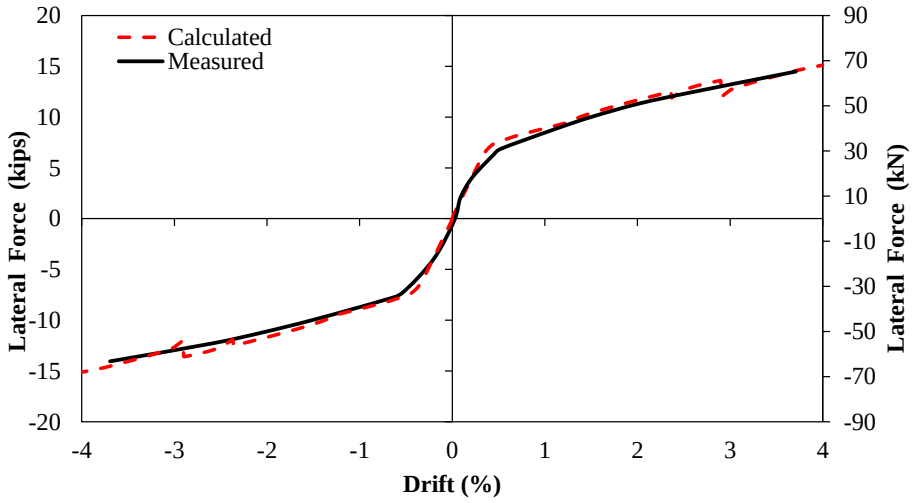

Figure 10. Measured and calculated force-displacement relationships for hybrid rocking column with external energy dissipaters (Test data from Marriott et al. [16] with the Authors' Permission)

3.3 Analysis results

Pushover analysis was carried out for all bridge column models to investigate the performance of the repairable bridge columns. Table 3 presents a summary of the analysis results and Fig. 11 to 14 show sample pushover relationships.
It can be seen that the pushover relationships vary significantly for different yielding lengths of the buckling restrained reinforcement (BRR-YL). Longer yielding lengths for BRR usually resulted in higher displacement capacities exceeding those of the corresponding conventional RC columns.

It was found that the precast columns with the proposed detailing can exhibit four times or higher displacement capacities than those for the corresponding conventional RC columns. This is especially true for columns with lower aspect ratios and lower axial load indexes. For instance, a precast column with

an aspect ratio of 4 and an axial load index of 5% exhibited a displacement ductility capacity of 15.4 when the yielding length of the BRR was equal to the analytical plastic hinge length (Fig. 11). The displacement capacity for the proposed bridge column was 5.1 times higher than that for the corresponding conventional RC bridge column.

Furthermore, columns with longer BRR and higher aspect ratios exhibited lower lateral load carrying capacities mainly due to significant $P-\Delta$ effect. Overall, the lateral load capacity of the proposed repairable columns are expected to be lower than the corresponding conventional columns due to the reduction in the column section close to the interface. For example, the column with an aspect ratio of 8, an axial load index of 15%, and the BRR yielding length equal to the analytical plastic hinge length (Fig. 14) showed 19% lower lateral load capacity compared to that of its corresponding conventional RC column (RC-AR8-ALI15-D3).

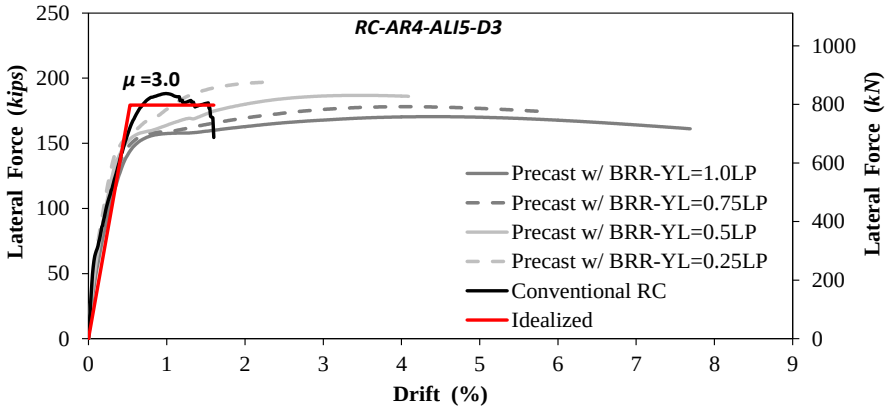

Figure 11. Pushover analysis for RC-AR4-ALI5-D3 and corresponding repairable precast column

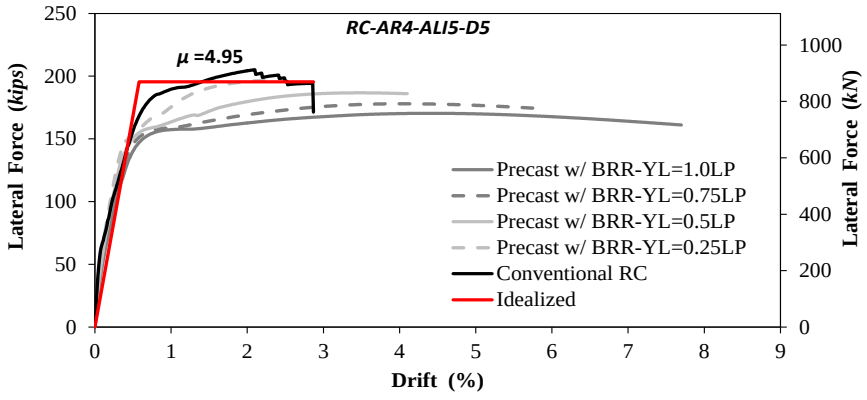

Figure 12. Pushover analysis for RC-AR4-ALI5-D5 and corresponding repairable precast column

Table 3. Summary of analysis results for repairable RC bridge columns

Column I.D	Drift Ratio Capacity, % (Displacement Ductility Capacity) BRR Yielding Length (BRR-YL)				Column Mode of Failure	
	$0.25L_p$	$0.5L_p$	$0.75L_p$	$1.0L_p$	Conventional	Novel
RC-AR4-ALI5-D3	2.29 (6.02)	4.09 (9.51)	5.88 (12.51)	7.69 (15.38)	Steel Bar Fracture	BRR Fracture
RC-AR4-ALI5-D5	2.30 (5.92)	4.10 (9.32)	5.90 (12.29)	7.70 (15.10)	Steel Bar Fracture	BRR Fracture
RC-AR4-ALI5-D7	2.32 (5.66)	4.12 (9.15)	5.90 (12.31)	7.70 (14.81)	Steel Bar Fracture	BRR Fracture
RC-AR4-ALI10-D3	2.37 (6.58)	4.24 (10.6)	6.10 (14.2)	7.94 17.28)	Steel Bar Fracture	BRR Fracture
RC-AR4-ALI10-D5	2.39 (6.29)	4.25 (10.37)	6.12 (13.61)	7.95 (16.93)	Steel Bar Fracture	BRR Fracture
RC-AR4-ALI10-D7	2.41 (6.18)	4.27 (9.93)	6.13 (13.63)	7.95 (16.57)	Steel Bar Fracture	BRR Fracture
RC-AR4-ALI15-D3	2.49 (6.92)	4.47 (11.19)	6.16 (14.34)	5.72 (12.18)	Steel Bar Fracture	BRR Fracture
RC-AR4-ALI15-D5	2.52 (6.63)	4.49 (10.7)	6.17 (14.04)	5.73 (11.95)	Steel Bar Fracture	BRR Fracture
RC-AR4-ALI15-D7	2.54 (6.35)	4.50 (10.47)	6.19 (13.47)	5.74 (11.73)	Steel Bar Fracture	BRR Fracture
RC-AR6-ALI5-D3	3.10 (5.34)	5.40 (8.85)	7.71 (12.24)	8.55 (12.96)	Core Concrete Failure	BRR Fracture
RC-AR6-ALI5-D5	3.13 (5. 21)	5.43 (8.62)	7.73 (12.08)	8.57 (12.79)	Core Concrete Failure	BRR Fracture
RC-AR6-ALI5-D7	3.14 (5.14)	5.44 (8.37)	7.75 (11.92)	8.57 (12.6)	Core Concrete Failure	BRR Fracture
RC-AR6-ALI10-D3	3.20 (6.15)	5.58 (10.34)	5.55 (9.57)	4.81 (7.76)	Core Concrete Failure	BRR Fracture
RC-AR6-ALI10-D5	3.24 (5.89)	5.61 (9.84)	5.57 (9.29)	4.82 (7.53)	Core Concrete Failure	BRR Fracture
RC-AR6-ALI10-D7	3.26 (5.82)	5.64 (9.73)	5.58 (9.15)	4.83 (7.43)	15% drop in Strength	BRR Fracture
RC-AR6-ALI15-D3	3.36 (6.72)	4.48 (8.46)	3.93 (6.78)	3.46 (5.41)	Core Concrete Failure	15% drop in Strength
RC-AR6-ALI15-D5	3.40 (6.42)	4.50 (8.04)	3.95 (6.59)	3.48 (5.27)	Core Concrete Failure	15% drop in Strength
RC-AR6-ALI15-D7	3.43 (6.24)	4.52 (7.8)	3.97 (6.41)	3.49 (5.21)	15% drop in Strength	15% drop in Strength
RC-AR8-ALI5-D3	3.91 (5.21)	6.71 (8.94)	6.74 (8.75)	5.82 (7.1)	15% drop in Strength	BRR Fracture
RC-AR8-ALI5-D5	5.38 (5.06)	6.75 (8.65)	6.76 (8.56)	5.83 (6.94)	Core Concrete Failure	15% drop in Strength
RC-AR8-ALI5-D7	5.44 (4.97)	6.78 (8.47)	6.78 (8.37)	5.85 (6.88)	15% drop in Strength	15% drop in Strength
RC-AR8-ALI10-D3	4.03 (6.2)	4.46 (6.66)	3.68 (5.18)	3.33 (4.21)	15% drop in Strength	15% drop in Strength
RC-AR8-ALI10-D5	4.08 (6)	4.49 (6.41)	3.71 (4.95)	3.35 (4.13)	15% drop in Strength	15% drop in Strength
RC-AR8-ALI10-D7	4.45 (4.54)	7.55 (7.78)	9.18 (9.56)	7.91 (7.98)	15% drop in Strength	15% drop in Strength
RC-AR8-ALI15-D3	3.78 (6.2)	3.24 (4.91)	2.83 (3.89)	2.72 (3.40)	15% drop in Strength	15% drop in Strength
RC-AR8-ALI15-D5	4.57 (5.37)	5.00 (5.88)	4.06 (4.51)	3.57 (3.71)	15% drop in Strength	15% drop in Strength
RC-AR8-ALI15-D7	5.71 (4.83)	8.64 (7.71)	8.20 (7.38)	6.80 (6.00)	15% drop in Strength	15% drop in Strength

Example of Specimen Identification: RC-AR4-ALI5-D3
RC: Reinforced Concrete Element, AR4: Aspect Ratio = 4,
ALI5: Axial Load Index = 5%, D5: Target Displacement Ductility Capacity = 5.

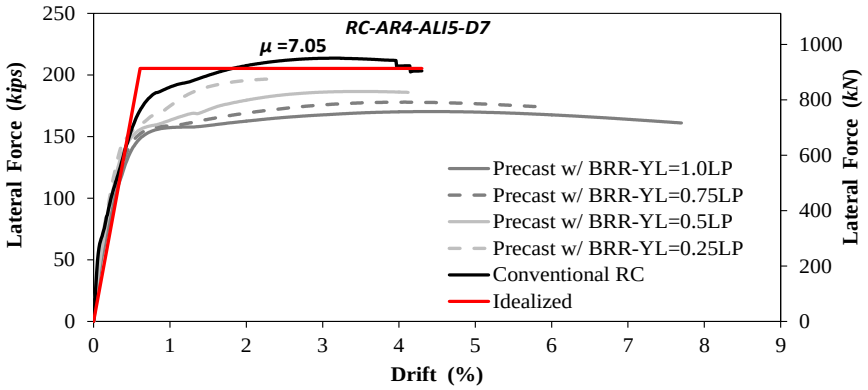

Figure 13. Pushover analysis for RC-AR4-ALI5-D7 and corresponding repairable precast column

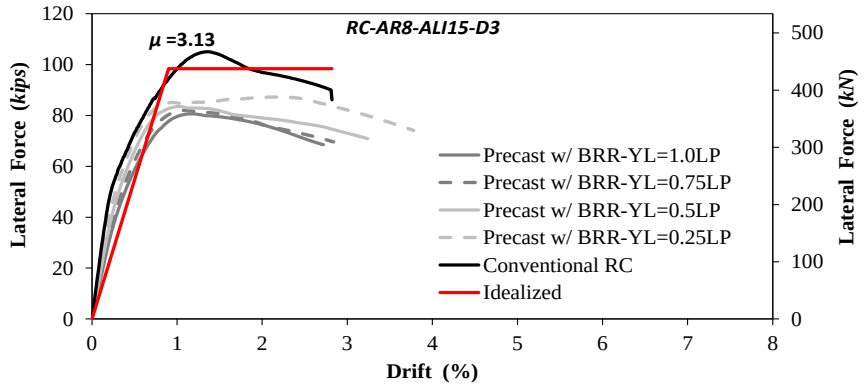

Figure 14. Pushover analysis for RC-AR8-ALI15-D3 and corresponding repairable precast column

Another finding was that a large displacement capacity can be achieved in the proposed repairable precast columns regardless of the confinement of the plastic hinge region. In other words, the displacement capacity of the proposed repairable columns is controlled by the yielding length of BRR not the confinement. For examples, the conventional columns of RC-AR4-ALI5-D3 and RC-AR4-ALI5-D5 and RC-AR4-ALI5-D7 (Fig. 11 to Fig. 14) are different because of their transverse reinforcement. Nevertheless, the precast version of these three RC columns is just one column. In these figures, it can be seen that the displacement capacities of the repairable precast columns exceeded those of the corresponding RC columns when the yielding length of BRR was equal to or higher than $0.5L_p$.

Furthermore, it was found that the bar fracture was the dominant mode of failure for the conventional and repairable bridge columns with the aspect ratio of 4. For the aspect ratio of 6, the common mode of failure for the conventional RC columns was the core concrete failure while fracture of BRR was more

often for the repairable precast columns. Significant $P-\Delta$ effect was seen for long columns with either conventional or the proposed detailing.

It is worth-mentioning that the failure of the core concrete is eliminated in the proposed repairable precast bridge columns by providing high confinement at the column ends and by placing a steel plate at the column to adjoining member interface to distribute the bearing stresses. It should be also noted that the present analytical study was only focused on the capacity of columns incorporating the proposed detailing to better understand their potentials.

However, extensive cyclic and dynamic analyses are needed to investigate all aspects of their seismic performance including demands. Large-scale testing is needed to experimentally validate the findings and to show the reparability of the proposed system.

4 CONCLUSIONS

A new construction and design approach was proposed in the present study to improve the seismic performance of RC bridge columns and to accelerate construction. The proposed novel column incorporates (1) pipe-pin connections to transfer plastic shear forces, (2) exposed buckling restrained reinforcement, BRR, to develop plastic moments and to be replaced after a severe event, and (3) detachable mechanical bar splices for quick replacement of damaged BRR. Based on the experimental and analytical investigations, the following conclusions can be drawn:

- Exposed BRR can be used as the main reinforcement of bridge columns if (1) the unrestrained length of BRR does not exceed half the bar diameter, and (2) the size of tube is determined based on the proposed design method for BRR.
- The proposed column detailing can increase the displacement capacity of bridge columns by a factor of four or more especially for columns with low aspect ratios and low axial loads.
- A BRR yielding length equal to the column analytical plastic hinge length results in large displacement capacities exceeding those of the corresponding conventional RC columns.
- Large displacement capacities can be achieved in the proposed repairable precast columns regardless of the confinement of the plastic hinge region.
- The proposed novel column is expected to be fast in construction since all components are prefabricated.
- The proposed novel column is expected to be repairable since the damage is limited to BRR, which can be detached after an event through the use of detachable mechanical bar splices. However, test data of large-scale specimens are needed to experimentally validate this feature.

Overall, the proposed novel column is expected to improve the seismic performance of bridges and to expedite the construction. The bridge total replacement after an earthquake is eliminated since bridge columns are repairable. Large-scale experimental studies are needed to confirm these findings before field deployment.

REFERENCES

[1] Mander, JB, Priesley, MJN, and Park, R, "Theoretical Stress Strain Model for Confined Concrete," Journal of Structural Engineering, ASCE, Vol. 114, No. 8, pp. 1804-1826, 1988.
[2] Stephens, MT, Lehman, DE, and Roeder, CW, "Concrete-Filled Tube Bridge Pier Connections for Accelerated Bridge Construction" California Department of Transportation, Report No. CA15-2417, 210 pp., 2015.
[3] Mirmiran, A, and Shahawy, M, "A New Concrete-Filled Hollow FRP Composite Column," *Composites*, Part B, Vol. 27B, pp. 263-268, 1996.
[4] AASHTO, "AASHTO Guide Specifications for LRFD Seismic Bridge Design, 2nd Edition" Washington, DC: American Association of State Highway and Transportation Officials, 2011.
[5] Buckle, IG, "Overview of Seismic Design Methods for Bridges in Different Countries and Future Directions," *11th World Conference for Earthquake Engineering*, Paper No. 2113, ISBN: 0080428223, 1996.
[6] AASHTO, "Guide Specifications for Seismic Isolation Design, 4th Edition," Washington, DC: American Association of State Highway and Transportation Officials, 2014.
[7] Tazarv, M, and Saiidi, MS, "Next Generation of Bridge Columns for Accelerated Bridge Construction in High Seismic Zones," CCEER Report No. 14-06, Center for Civil Engineering Earthquake Research, University of Nevada, Reno, Nevada., 400 pp., 2014.
[8] Mander, JB, Cheng, CT, "Seismic Resistance of Bridge Piers Based on Damage Avoidance Design," NCEER-97-0014, National Center for Earthquake Engineering Research, State University of New York at Buffalo, 130 pp., 1997.
[9] Varela, S, and Saiidi, MS, "Resilient Deconstructible Columns for Accelerated Bridge Construction in Seismically Active Areas," *Journal of Intelligent Material Systems and Structures*, DOI: 10.1177/1045389X16679285, 2016.
[10] Guerrini, G, Restrepo, JI, Massari, M, and Vervelidis, A, "Seismic Behavior of Posttensioned Self-Centering Precast Concrete Dual-Shell Steel Columns," *Journal of structural engineering*, ASCE, Vol. 141, No. 4, 04014115, 2014. .
[11] Yang, Y, Sneed, LH, Morgan, A, Saudi, MS, and Belarbi, A, "Repair of RC Bridge Columns with Interlocking Spirals and Fractured Longitudinal Bars-An Experimental Study," Construction and Building Materials, Vol. 78, pp. 405-420, 2015.
[12] White, S. Palermo, A. "Quasi-Static Testing of Posttensioned Nonemulative Column-Footing Connections for Bridge Piers," Journal of Bridge Engineering, ASCE, Vol. 21, No. 6, 13 pp, 2016.
[13] Tazarv, M. and Saiidi, M.S. "Seismic Design of Bridge Columns Incorporating Mechanical Bar Splices in Plastic Hinge Regions," Engineering Structures, DOI: 10.1016/j.engstruct.2016.06.041, Vol. 124, pp. 507-520, 2016.
[14] AASHTO, "AASHTO LRFD Bridge Design Specifications, 7th Edition" Washington, DC: American Association of State Highway and Transportation Officials, 2014.
[15] Zaghi, A, and Saiidi, MS, "Seismic Design of pipe pin connections in Concrete Bridges," CCEER Report No. 10-01, Center for Civil Engineering Earthquake Research, University of Nevada, Reno, Nevada, 2010.
[16] Marriott, D, Pampanin, S, and Palermo, A, "Quasi-Static and Pseudo-Dynamic Testing of Unbonded Posttensioned Rocking Bridge Piers with External Replaceable Dissipaters,"

Earthquake Engineering & Structural Dynamics, Vol. 38, No. 3, pp. 331-354, 2009.
[17] Marriott, D, Pampanin, S, and Palermo, A, "Biaxial Testing of Unbonded Post-tensioned Rocking Bridge Piers with External Replaceable Dissipaters," *Earthquake Engineering & Structural Dynamics*," Vol. 40, No. 15, pp. 1723-1741, 2011.
[18] Pampanin, S, "Emerging Solutions for High Seismic Performance of Precast/Prestressed Concrete Buildings." *Journal of Advanced Concrete Technology*, Vol. 3, No. 2, pp. 207-223, 2005.
[19] Tuhin, IA, "Application of New Materials and Innovative Detailing for Reinforced Concrete Structures," MSc thesis, South Dakota State University, Brookings, South Dakota, 181 pp., 2016.
[20] Sarti, F, Palermo, A, and Pampanin, S, "Fuse-Type External Replaceable Dissipaters: Experimental Program and Numerical Modeling," *Journal of Structural Engineering*, ASCE, 04016134, 2016.
[21] OpenSees, "Open System for Earthquake Engineering Simulations," Version 2.4.6, Berkeley, CA, 2015.